J Mol Model (2012) 18:3311–3320
DOI 10.1007/s00894-011-1350-7

ORIGINAL PAPER

Anion recognition based on halogen bonding: a case study of macrocyclic imidazoliophane receptors

Yunxiang Lu · Haiying Li · Xiang Zhu · Honglai Liu · Weiliang Zhu

Received: 15 November 2011 / Accepted: 29 December 2011 / Published online: 18 January 2012

Abstract The structures and properties of noncovalent interactions involving three imidazoliophane receptors **1–3** and halide anions have been investigated by means of density functional theory calculations. To account for the influence of the solvent environment, the implicit polarized continuum model was also employed. For the halogenated cyclophane receptors **1** and **2**, the halide ions are held by a bidentate array of halogen bonds (C−Br/C−I...X^-), while multiple hydrogen-bonding interactions (C−H...X^-) are present in the complexes of the nonhalogenated macrocyclic receptor **3**. To accommodate the negatively charged guest anions, the structures of **1** and **2** fully reorganize into a calix-like shape, while both the imidazole and benzene rings in **3** tend to point towards the anions and thus rotate to form a cage-like shape. In both the gas phase and aqueous solution, the binding affinities of the anions for halogen-bonding receptors **1** and **2** become stronger than those for hydrogen-bonding receptor **3**. The results reported here should prove to be of great value in the design and synthesis of effective and selective anion receptors based on halogen bonding.

Keywords Anion receptors · Noncovalent interactions · Binding behaviors · Binding affinity

Introduction

The design and synthesis of artificial receptors with high affinity and selectivity for specific anions is an area of intense current interest, due to the important roles of negatively charged species in chemical, biological, medical, and environmental processes [1–12]. Hydrogen bonding has been, by far, the noncovalent interaction most frequently employed in the design of anion receptors [13–18]. However, many anion receptors that rely upon other intermolecular forces, including complementary electrostatic, Lewis acid-base, and anion–π interactions, have been developed in recent years [19–25]. Such studies have provided insight into the interactions utilized and thus offer new strategies to achieve the recognition and binding of anions.

Halogen bonding, a specific noncovalent interaction in which halogen atoms act as electrophiles, has been the subject of numerous studies in such diverse fields as crystal engineering, supramolecular architectures, and biological design [26–34]. As demonstrated by Murray and coworkers, covalently bound halogens X display a region of positive electrostatic potential (the so-called sigma-hole) centered around the extension of the R−X bonds, which primarily accounts for the directionality of halogen bonding [31, 35–39]. To date, most applications of halogen bonding have involved the solid state; evidence of this interaction in a solution phase is rare [40–45]. The recognition of anions in solution by halogen bonding is only now being uncovered, and some anion receptors based on this specific interaction have been developed [46–50]. For example, two kinds of receptors capable of tightly binding halide ions

Electronic supplementary material The online version of this article (doi:10.1007/s00894-011-1350-7) contains supplementary material, which is available to authorized users.

Y. Lu (✉) · H. Li · X. Zhu · H. Liu
Key Laboratory for Advanced Material and Department of Chemistry, East China University of Science and Technology, Shanghai 200237, People's Republic of China
e-mail: yxlu@ecust.edu.cn

W. Zhu
Drug Discovery and Design Center, Shanghai Institute of Materia Medica, Chinese Academy of Sciences, Shanghai 201203, People's Republic of China

via multidentate halogen bonds have been reported recently [46, 47], and these represent the first macrocyclic systems in which the cooperative behavior of multiple halogen bond donors is applied to achieve high selectivity and affinity in dilute solution. Furthermore, to improve the anion-recognition capabilities of interlocked binding pockets, halogen-bonding rotaxane host systems based upon halogenated triazolium and imidazolium axles (a central shaft for a rotating wheel or gear) have been developed [48, 49]. Very recently, Taylor and co-workers explored anion recognition through a combination of halogen and hydrogen bonding [51]. Nonetheless, in contrast to hydrogen bonding, the use of solution-phase halogen bonding to control and facilitate anion recognition is still in its infancy.

A common approach to preparing molecules that coordinate with anions is to add hydrogen bond donor groups, D–H, to an organic scaffold, thus yielding receptors that can interact with anions via hydrogen bonding [10, 11, 52, 53]. Over the past several years, a number of hosts containing a variety of D–H groups, such as amides, thioamides, sulfonamides, amines, pyrroles, imidazolium cations, ureas, thioureas, and guanidinium cations, have been extensively investigated from both experimental and theoretical viewpoints [12, 54–59]. For example, in 2008, Cavallotti et al. examined the properties of nonbonding interactions involving guanidinium-functionalized hosts and carboxylate substrates using a combination of ab initio and molecular dynamics approaches [60]. More recently, the binding behaviors of 27-membered macrocyclic triureas towards several anions through multiple hydrogen-bonding interactions were studied with density functional theory (DFT) calculations [61]. However, to the best of our knowledge, few theoretical studies concerning halogen-bonding-based macrocyclic receptors and their binding behaviors with anions have been reported up to now. It is well documented that the strength of halogen bonding is comparable to that of hydrogen bonding, but it has a more strictly linear geometry and different steric requirements [26]. Therefore, the incorporation of halogen atoms into anion–receptor frameworks should significantly influence the binding behavior of the receptor from both geometric and energetic perspectives. Considering the increasing importance of halogen bonding in the development of effective anion receptors, it is necessary to elucidate the binding properties of halogenated macrocyclic receptors with guest anions from a theoretical point of view.

In this paper, we present a quantum chemical study of the structures and characteristics of nonbonding interactions involving three imidazoliophane receptors **1**–**3** (hexafluorophosphate salts, see Fig. 1) and halide anions (F^-, Cl^-, Br^-, I^-). The X-ray crystal structure of the bromoimidazoliophane receptor **1** has already been determined [47]. The host molecule **2** is derived from **1** by substituting the two Br atoms on the imidazole rings with I atoms. The association constants for bromide receptor **1** and its protic form **3** with different halide ions have been experimentally determined in competitive aqueous media (9:1 CD_3OD/D_2O), and the halide-binding strength decreases according to the trend bromide > iodide > chloride > fluoride ions when using the brominated receptor **1** [47]. For the halogenated receptors **1** and **2**, halide ions should be held by a bidentate array of halogen bonds (C^2–Br/ C^2–I...X^-), while multiple hydrogen-bonding interactions (C^2–H/C^8–H...X^-) are expected to occur in the systems of the nonhalogenated receptor **3** [47]. It should be noted that, in recent years, many exciting and significant results have been obtained by applying new imidazolium receptors to various anionic targets, such as ATP, DNA, and also simple anions [62].

Computational details

The geometries of all the receptors and anion complexes were fully optimized in vacuum using Becke's three-parameter exchange functional combined with the gradient-corrected correlation functional of Lee, Yang and Parr (B3LYP) [63, 64]. Unless otherwise specified, no geometry and symmetry constraints were imposed during the calculations. The B3LYP method has recently been demonstrated to provide reasonably good descriptions of charged strong halogen bonds [65]. Also, this hybrid functional has been widely utilized in the study of nonbinding interactions between macrocyclic receptors and various anions [60, 61]. The cc-pVDZ-PP basis set—which uses pseudopotentials to describe the inner core orbitals—was employed for iodine, while the cc-pVDZ basis set was applied for all other atoms [66]. Frequency calculations were carried out at the same theoretical level to confirm that the structures obtained correspond to energetic minima.

The interaction energy (ΔE_{int}) was defined as the difference between the total energy of the complex and the sum of the total energies of the minimum geometry of the receptor and the halide ions. The basis set superposition error (BSSE) was corrected by the standard counterpoise (CP) method of Boys and Bernardi [67]. The structural deformation energy (ΔE_{deform}) was estimated as the difference between the total energy of the binding geometry of the receptor on one hand and that of the minimum geometry on the other. To investigate the capacity of B3LYP/cc-pVDZ to accurately predict the geometries and energetics of the macrocyclic systems under study, calculations were also performed on the simple complexes of ion pair **4**, composed of a bromoimidazole cation and a PF_6^- anion (see Fig. 1 of the "Electronic supplementary material," ESM) at the B3LYP and second-order Moller–Plesset perturbation theory (MP2) [68] levels with the same or a larger basis set. For some macrocyclic

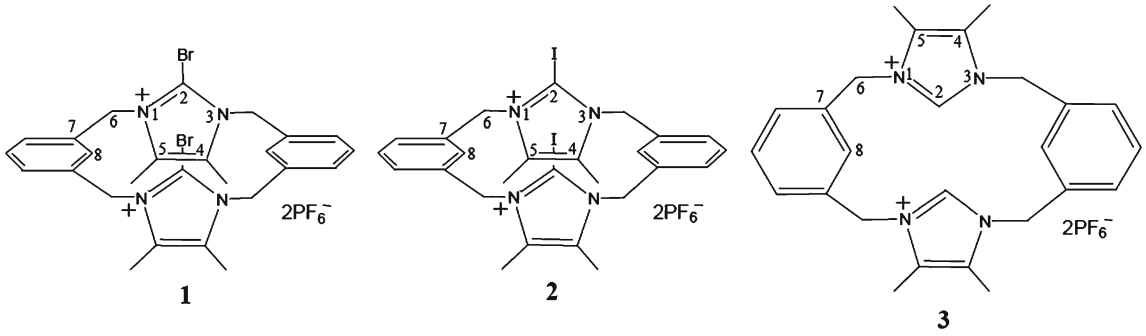

Fig. 1 Chemical structures of the three imidazoliophane receptors **1–3** under study

anion complexes, single-point energy calculations using the B3LYP/cc-pVDZ geometries were carried out at the B3LYP/6-31++G(d,p)-aVDZ level (aug-cc-pVDZ for Cl, Br, and I atoms, and 6-31++G(d,p) for the other atoms) to check the convergence.

Calculations in aqueous solution were performed via the standard polarizable continuum model (PCM) at the B3LYP/cc-pVDZ level of theory [69–71]. The molecular cavity was constructed by the united atom topological model (UAO) employing the default radii [69]. This implicit solvation approach has been successfully used to investigate solvent effects on halogen bonding with a broad range of strengths [65]. The optimized geometries in the gas phase were utilized as starting points for the optimizations in water with a dielectric constant of 78.39. All of the calculations reported in this work were carried out with the help of the Gaussian 03 suite of programs [72].

Results and discussion

Binding geometries and energies for the small complexes of ion pair 4

The B3LYP/cc-pVDZ optimized structures for the simple complexes of brominated ion pair **4** with halide ions (**4**−F^-, **4**−Cl^-, **4**−Br^- and **4**−I^-) are displayed in Fig. 1 of the ESM. The key geometrical parameters and interaction energies for these systems calculated at various levels are summarized in Table 1 of the ESM. For the most stable geometry of ion pair **4**, the PF_6^- anion is most favorably located above the imidazole ring, as it forms multiple F...H hydrogen bonds with methyl moieties on the ring, which agrees well with the X-ray crystallographic structure of the brominated macrocyclic receptor **1** [47]. The optimized equilibrium C−Br...X^- contacts at the three theoretical levels are essentially linear (≈ 180°); all the predicted intermolecular distances are significantly smaller than the sums of the van der Waals (vdW) radii of the atoms involved [73], quite similar to the structural characteristics of conventional strong halogen bonds [26, 65]. As compared to the other two theoretical approaches used, B3LYP/cc-pVDZ yields rather shorter halogen bonding lengths, consistent with the more negative interaction energies estimated at this level of theory. However, the differences in the intermolecular distances found at the B3LYP/cc-pVDZ and B3LYP/aug-cc-pVDZ or MP2/cc-pVDZ levels are less than 0.1 Å; the intermolecular separations for the complexes obtained with the three methods increase in the same order: $F^- < Cl^- < Br^- < I^-$.

Not unexpectedly, the B3LYP/cc-pVDZ method overestimates the interaction energies to some extent, especially for **4**−F^-. A previous study of the molecular recognition of resorcin[4]arene receptors also revealed that compared to MP2, B3LYP predicts much greater interaction energies for the F^- complexes [74]. Nonetheless, the order of halide ion affinity ($F^- > Cl^- > Br^- > I^-$) is the same, whichever of the three methods is used, which accords with the increase in the intermolecular distances for the X^- complexes. At this point, it is worth mentioning that the interaction energies calculated with B3LYP/cc-pVDZ correlate well with those of B3LYP/aug-cc-pVDZ and MP2/aug-cc-pVDZ; the linear correlation coefficients (R^2) are both as high as 0.996. Therefore, the B3LYP/cc-pVDZ calculations are reliable for predicting the relative order of halide ion affinity strength. Considering the large size of the macrocyclic systems under study, which prohibits the use of high-level theoretical methods, the hybrid B3LYP functional with the medium-sized basis set cc-pVDZ was employed in the calculations of imidazoliophane receptors and complexes of them with X^-.

Upon performing B3LYP/aug-cc-pVDZ calculations, the interaction energies of these complexes were found to range from −23.44 kcal mol^{-1} to −48.33 kcal mol^{-1}, thus indicating strong Br...X^- interactions in these systems. In particular, halogen bonds in the brominated ion pair complexes become stronger than those in iodo-perfluorocarbon (I-PFC) systems [65]. For example, at the same theoretical level, the interaction energies for the complexes of iodo-pentafluorobenzene with Cl^-, Br^-, and I^- are estimated to be in the range −20.06 to −26.34 kcal mol^{-1} [65]. It is well known that the major

breakthrough in the application of halogen bonding in crystal engineering was based on the organic supramolecular architectures derived from specific synthons containing I-PFCs [26], because of their effectiveness at producing strong halogen bonds. Clearly, halogen bonding based on halogenated imidazolium ion pairs shows great potential for application in the design and synthesis of novel and high-value functional materials. The calculations presented here may also provide some useful information when developing new and task-specific imidazolium ionic liquids.

Conformational features of receptors 1–3

In Beer's work, single X-ray crystals for the *anti* and *syn* isomers of the brominated receptor **1** were both obtained [47]. The two structures can also be located using the B3LYP/cc-pVDZ method, as graphically depicted in Fig. 2. In the *syn* structure, the two bromoimidazolium groups are almost parallel to each other, with the Br...Br distance being equal to 4.68 Å; the two PF_6^- anions are located over the imidazole rings and form multiple F...H hydrogen bonds with methyl groups on the rings—very similar to the structure of ion pair **4**. The *anti* structure has the same arrangement; however, the two Br atoms on the imidazole rings are in the *anti* position [*d*(Br...Br) = 6.28 Å]. A comparison between the calculated geometrical data and the X-ray crystal structures reveals that the calculated structures compare relatively well to the X-ray structures [47]. The computed bond lengths of the imidazole and benzene rings are within 0.05 Å of the X-ray values, and the differences between the predicted bond angles of the rings and experimental values are less than 3°. In the case of the *anti* isomer, each bromoimidazolium group can interact with one halide ion, whereas for the *syn* isomer, bidentate halogen bonds between two bromoimidazolium moieties and one halide ion can be expected. At the B3LYP/cc-pVDZ level, the *anti* structure is calculated to be only about 0.80 kcal mol^{-1} more stable than the *syn* structure. Thus, in the

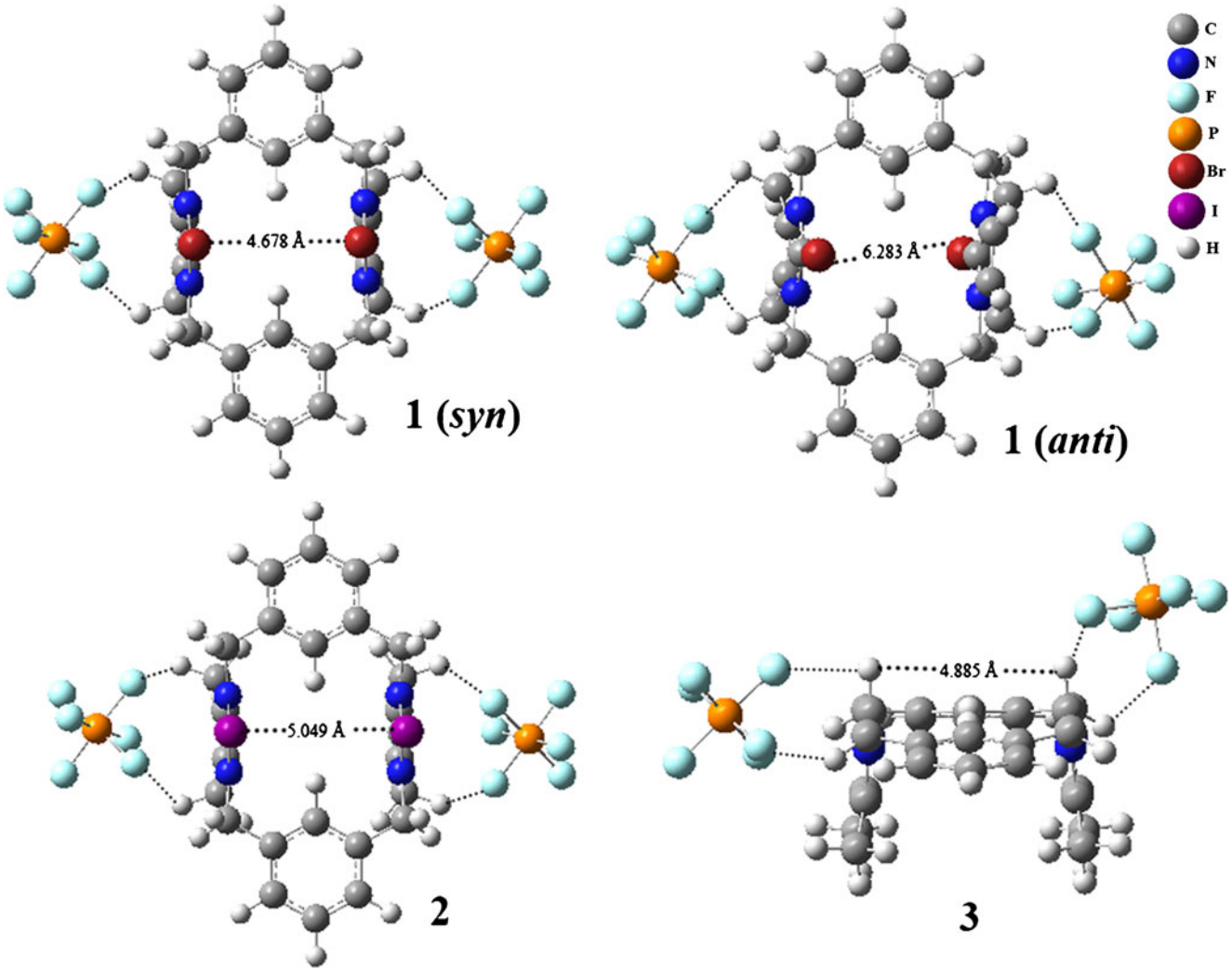

Fig. 2 The structures of receptors **1–3** optimized at the B3LYP/cc-pVDZ level

following discussion, the *syn* structures of the receptors that can form bidentate halogen bonds with halide ions are considered.

As mentioned above, host molecule **2** is built from the brominated receptor **1**, so the optimized geometries of the two halogenated receptors are quite similar to one another. Nevertheless, due to the larger size of the I atoms compared to the Br atoms, as well as the greater steric repulsion between them, the separation between the two parallel imidazolium groups in **2** is larger than in **1** (5.05 Å vs 4.68 Å). As shown in Fig. 2, the structure of the nonhalogenated receptor **3** is strikingly different to those of the halogenated ones: the two PF_6^- anions in this structure prefer to approach the C^2–H fragments asymmetrically, which can be explained by the fact that, compared with the methyl groups on the imidazole ring, the C^2–H should form stronger H...F interactions with PF_6^-. The shortest H(C^2)...F distances amount to 2.54 Å and 1.96 Å, respectively, for the two PF_6^- anions, reflecting the asymmetric structure of receptor **3**, in which one PF_6^- anion is located above the C^2–H fragment while the other tends to move slightly below the fragment. This finding is presumably ascribed to steric demands and electrostatic repulsion, which prevents the two PF_6^- anions approaching the C^2–H fragments in a symmetric way. In fact, the dipole moment of **3** is computed to be 16.48 D, considerably larger than those of **1** and **2** (2.43 D and 5.04 D).

Binding geometries and energetics for the complexes of receptors 1–3

The optimized geometries of the anion complexes of receptors **1–3** are depicted in Figs. 3, 4, and 5. The key structural parameters and dipole moments of these complexes are given in Tables 1 and 2. As anticipated, for the halogenated receptors **1** and **2**, halide ions are held by two equivalent X... X^- interactions that are less linear than those in the simple complexes of ion pair **4**. Moreover, the intermolecular X... X^- distances in the macrocyclic systems appear to be much greater than those for the corresponding small complexes. For example, at the B3LYP/cc-pVDZ level, the Br...Br^- distances in **4**–Cl^- and **1**–Cl^- are estimated to be 2.66 Å and 2.88 Å, respectively, while the C–Br...Br^- angles amount to 176° and 162° for the two complexes. Obviously, individual halogen bonds in the macrocyclic systems are much weaker than those in the complexes of ion pair **4**. This is not surprising, due to the effect of the steric hindrance of the two imidazole rings as well as electrostatic repulsion between the two electropositive halogen atoms. The F^- complexes show the shortest intermolecular distances (about 2.40 Å), a reduction of approximately 30% compared to the sum of the vdW radii of the atoms involved [73], indicating that the strongest halogen bonds occur in the F^- systems (vide infra). The intermolecular distances in the complexes tend to decrease in the order $I^- > Br^- > Cl^- > F^-$, which has been widely established in many macrocyclic receptor systems, such as triazolophanes, tetramine hexaether, and triurea [61, 75, 76].

Inspection of Fig. 5 reveals that in the complexes of the nonhalogenated receptor **3**, four hydrogen-bonding interactions (two C^2–H...X^- and two C^8–H...X^- hydrogen bonds) are present. These nonbonding interactions have long been recognized and explored, because of their decisive roles in receptor–anion binding [77–79]. Due to the small size of the fluoride ion and the formation of strong H...F^- hydrogen bonds, F^- resides at the center of the cavity, while the other three anions undergo a slight departure from the center, as

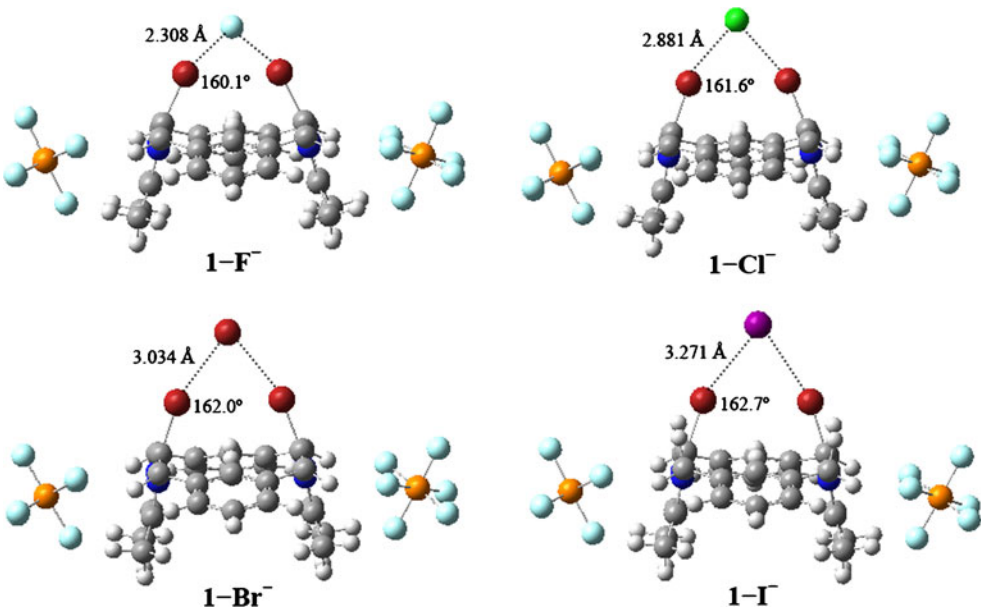

Fig. 3 Optimized structures of the complexes of receptor **1** at the B3LYP/cc-pVDZ level

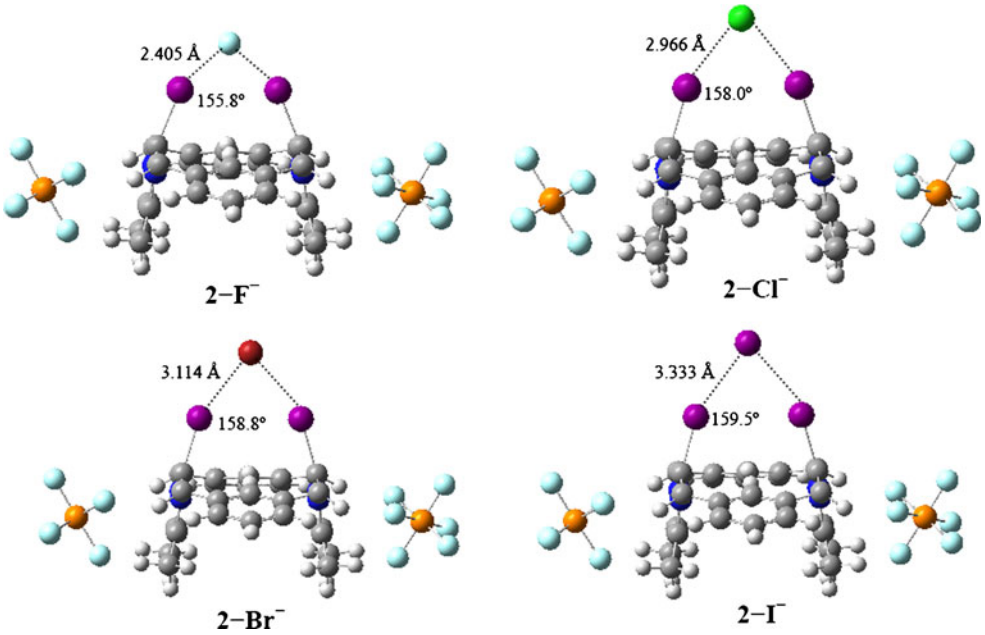

Fig. 4 Optimized structures of the complexes of receptor **2** at the B3LYP/cc-pVDZ level

shown in Fig. 2 of the ESM. In all cases, the benzene C^8–H...X^- hydrogen bonds appear to be weaker than the imidazolium C^2–H...X^- interactions, as indicated by the much longer H(C^8)...X^- distances. Therefore, the major driving force for complexation between receptor **3** and halide ions should come from the two imidazole C^2–H...X^- hydrogen bonds, while the two benzene C^8–H...X^- interactions also contribute to the binding of the anions. The participation of benzene hydrogen bonding in anion binding has also been demonstrated in the recent literature [80].

For the anion complexes of **1** and **2**, the formation of X...X^- halogen bonds affects the interactions between PF_6^- and imidazolium groups only marginally; multiple F...H hydrogen bonds between PF_6^- and the methyl moieties on the imidazole rings were also discovered. However, when guest anions are present in the nonhalogenated receptor **3**, the PF_6^- group above the C^2–H fragment tends to be located

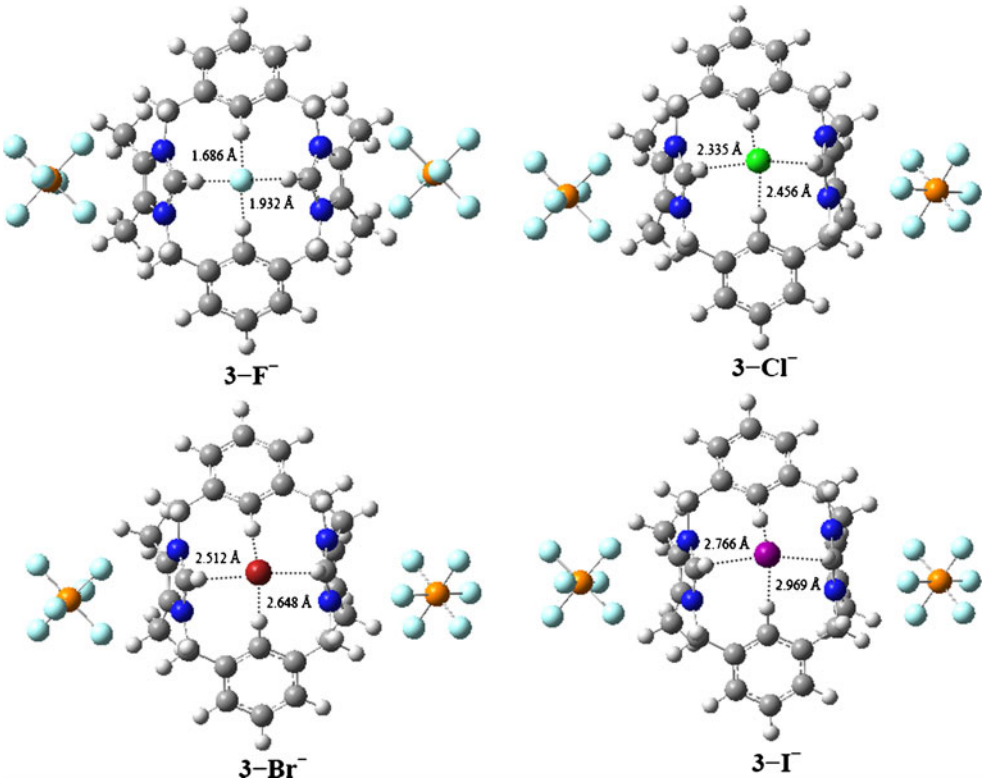

Fig. 5 Optimized structures of the complexes of receptor **3** at the B3LYP/cc-pVDZ level

Table 1 Selected structural parameters and dipole moments for the complexes of **1** and **2**[a]

Complexes	μ	d(X...X$^-$)	$\angle$(C^2–X...X$^-$)	Δd (C^2–X)[b]	d(X(C^2)...X(C^2))	d(H(C^8)...H(C^8))	d(C^2...C^2)
1–F$^-$	5.98	2.308	160.1	0.062	3.282	3.077	4.934
1–Cl$^-$	8.77	2.881	161.6	0.052	3.585	3.069	4.901
1–Br$^-$	8.08	3.034	162.0	0.056	3.649	3.043	4.902
1–I$^-$	8.07	3.271	162.7	0.057	3.742	3.050	4.903
2–F$^-$	1.97	2.405	155.8	0.079	3.466	2.952	5.078
2–Cl$^-$	4.45	2.966	158.0	0.073	3.733	2.938	4.998
2–Br$^-$	3.66	3.114	158.8	0.078	3.784	2.938	4.995
2–I$^-$	3.17	3.333	159.5	0.084	3.867	2.936	4.988

[a]Distances are given in angstroms, angles in degrees, and dipole moments in debyes

[b]The variation in the C^2–X bond length upon complexation

over the imidazole ring, much like the other PF_6^- (see Fig. 5). In fact, the dipole moments of the complexes of **3** are calculated to be considerably smaller than that of the free receptor. Apparently, the presence of halide ions moves the PF_6^- anion away from the C^2–H fragment, on account of electrostatic repulsion between the halide ions and the PF_6^-.

The variation in the C–H/C–X bond lengths upon complex formation is an important structural feature of hydrogen and halogen bonding. It can be readily appreciated from Table 1 that all the imidazolium C^2–X distances increase by about 52~84 mÅ upon complexation, consistent with the weakening of the C^2–X bond by electron donation from halide anions into the C^2–X antibonding orbital. Notably, the C–I bond in the systems of **2** undergoes more pronounced elongation than the C–Br bond in the complexes of **1**, thereby suggesting stronger I...X$^-$ halogen bonds in the former cases. Similarly, the strengths of the C–H...X$^-$ hydrogen bonds in the complexes of **3** can also be inferred from the increases in the C–H bond distances. As shown in Table 2, larger elongations of the C^2–H bond relative to C^8–H indicate stronger C^2–H...X$^-$ hydrogen bonds in these systems.

To accommodate the negatively charged guest anions, the structures of the halogen-bonding receptors **1** and **2** fully reorganize into a calix-like shape (the imidazolium-imidazolium plane angles = 20~50°), attracting the two positively charged halogen atoms more closely, as shown in Figs. 3 and 4. Moreover, the X(C^2) atoms do not seem to be in the imidazolium plane; the X–C^2–N^1–C^5 dihedral angles amount to approximately 165°. Clearly, the X(C^2) atoms tend to point towards halide anions by forming strong X...X$^-$ interactions, whereas the two imidazole rings are unlikely to rotate completely inwards due to high steric repulsion between them. Not surprisingly, structural variations of the F$^-$ complexes are much more pronounced than the systems of other halide anions, because the host cavity is relatively large for the fluoride ion (see Fig. 3 of the ESM). In fact, the deformation energies for the F$^-$ complexes are substantial, ranging from 15.08 kcal mol^{-1} to 19.02 kcal mol^{-1} (cf. Table 3), which confirms that huge changes in distances, angles, and conformations are required to achieve strong binding of F$^-$. Similar to receptors **1** and **2**, the H(C^2)...H(C^2) distances in the hydrogen-bonding receptor **3** are also shortened by 0.52~1.70 Å upon complexation. Nonetheless, the distances between the two H(C^8) atoms in the complexes of **3** become somewhat larger, as a result of the formation of weak C^8–H...X$^-$ interactions. As displayed in Fig. 5, when guest anions are present, both the imidazole and benzene rings in receptor **3** tend to point towards the anions and thus rotate to form a cage-like shape.

Calculated energetic data for the studied complexes are collected in Table 3. At the B3LYP/cc-pVDZ level, the predicted interaction energies for the anion complexes under investigation are within the range −39.02 to −84.30 kcal

Table 2 Selected structural parameters and dipole moments for the complexes of **3**[a]

Complexes	μ	d(H(C^2)...X$^-$)		$\angle$(C^2–H ...X$^-$)		d(H(C^8)...X$^-$)		$\angle$(C^8–H...X$^-$)		Δd (C^2–H)[b]	Δd (C^8–H)[c]	d(H(C^2)...H(C^2))	d(H(C^8)...H(C^8))	d(C^2...C^2)
3–F$^-$	9.55	1.686	1.688	148.7	148.6	1.932	1.939	176.0	175.7	0.034	0.012	3.182	3.272	4.619
3–Cl$^-$	11.53	2.335	2.392	144.8	140.1	2.456	2.570	165.8	167.7	0.012	0.006	4.063	3.311	4.878
3–Br$^-$	11.01	2.512	2.578	144.9	140.1	2.648	2.771	159.8	162.2	0.010	0.005	4.216	3.274	4.912
3–I$^-$	10.19	2.766	2.869	145.4	139.2	2.969	3.087	149.5	155.1	0.008	0.003	4.415	3.205	4.945

[a] Distances are given in angstroms, angles in degrees, and dipole moments in debyes

[b] The mean variation in the two C^2–X bond lengths upon complexation

[c] The mean variation in the two C^8–H bond lengths upon complexation

Table 3 Calculated energetic data for the complexes under study[a]

Complexes	ΔE_{int}	ΔE_{deform}	ΔH^{gas}	ΔG^{gas}	ΔE^{sol}
1–F^-	−74.93 (−62.86)	15.08	−106.02	−94.99	−31.04
1–Cl^-	−51.17 (−45.37)	8.26	−56.41	−46.25	−3.91
1–Br^-	−47.50 (−41.55)	7.70	−51.94	−42.16	−4.07
1–I^-	−41.62 (−37.86)	6.69	−44.04	−34.64	−1.74
2–F^-	−84.30 (−73.93)	19.52	−119.38	−109.76	−38.45
2–Cl^-	−60.81 (−55.23)	11.54	−67.49	−58.63	−7.24
2–Br^-	−57.35 (−51.57)	10.90	−63.19	−54.65	−7.44
2–I^-	−51.69 (−47.76)	9.84	−54.92	−46.83	−5.41
3–F^-	−73.32	17.54	−123.78	−114.71	−42.86
3–Cl^-	−50.56	11.15	−61.03	−53.30	−3.39
3–Br^-	−45.72	10.26	−54.84	−47.27	−2.42
3–I^-	−39.02	9.37	−44.39	−37.29	0.69

[a] All values are given in kilocalories per mole. ΔE^{sol} is the binding energy for the complexes in water. The values in parentheses are the binding energies calculated with B3LYP/6-31++G(d,p)-aVDZ

mol^{-1} in gas phase. Relative to the systems of **3**, the computed interaction energies for the complexes of **1** and **2** show an increase in absolute value. Therefore, the binding affinities of the anions strengthen with the addition of halogen atoms to the imidazole rings of the cyclophane receptor. As expected, the interaction energies of the complexes of **2** are calculated to be about 10 kcal mol^{-1} greater than those of the systems of **1**, thus suggesting stronger I...X^- halogen bonds in the former. From Table 3, it is also seen the binding affinities of anions for receptors **1**–**3** decrease in the same order $F^- > Cl^- > Br^- > I^-$ in vacuum, which has been widely established in many macrocycilc systems with halide ions [61, 75, 76]. Additionally, there is a good correlation ($R^2 = 0.985$) between the interaction energies attained with B3LYP/cc-pVDZ and B3LYP/6-31++G(d,p)-aVDZ, further validating the reliability of B3LYP/cc-pVDZ for predicting the relative order of halide anion affinity strength.

According to the above discussion, the incorporation of halogen atoms into the bis(imidazolium) macrocyclic framework leads to disparate conformations of the receptor to accommodate halide ions as well as entirely different binding behaviors towards the anions, enabling halide ion recognition to take place by pure halogen-bonding interactions. Moreover, with the presence of halogen atoms in the imidazole rings, the binding affinity of halide ions for the cyclophane receptor improves. Clearly, halogen-bonding-based receptors have great potential applications in anion recognition.

Solvent effect on binding properties

To explore the effects of solvent on the binding affinities of anions, all of the X^- complexes under study were examined in aqueous solution using the implicit PCM method. The key geometrical parameters for the complexes optimized in water are collected in Tables 2 and 3 of the ESM. As can be seen, all of the intermolecular X...X^- distances in the complexes of **1** and **2** are elongated by 0.10~0.40 Å due to solvent effects, while halogen-bonding angles remain almost unchanged in water [$\angle(C^2{-}X...X^-) \approx 160°$]. Clearly, X...$X^-$ halogen bonds are destabilized in aqueous solution [65]. Due to the increased X...X^- distances, the separations between the two imidazole rings in the complexes increase in water. However, the distances between the two H(C^8) atoms on the phenyl groups change slightly in water, and all the trends for the intermolecular distances observed in the gas phase are reproduced in aqueous media. Due to solvent effects, all the H...X^- distances in the systems of **3** are found to increase as well, thereby suggesting the weakening of hydrogen-bonding interactions in solution [61, 76]. In a water environment, imidazolium H(C^2)...X^- hydrogen bonds are less linear, but it has shorter H...X^- distances than that of benzene H(C^8)...X^-, similar to those seen in vacuum.

The interaction energies of all the complexes under investigation are greatly reduced by solvent effects (see Table 3). Hence, the strengths of the halogen and hydrogen bonds in these systems tend to significantly weaken in water, which agrees well with the elongation of intermolecular distances. The interaction energies of the F^- complexes are predicted to be more negative than those of the Cl^-, Br^-, and I^- systems, indicating that the F^- ion binds more strongly with the receptors in water. However, the titration experiments in aqueous media showed no detectable evidence of the binding of F^- ion by the macrocyclic receptors **1** and **3** [47]. This discrepancy can be ascribed to the rarity of a "free" F^- ion under normal experimental conditions. In fact, the hydration of fluoride ion appears to be very strong relative to other halide ions [75]. It is worth mentioning here that in a water environment, the calculated interaction energies of the complexes of **2** are somewhat greater than those for the systems of **1** and **3**. In this regard, the binding affinities of halide anions in solution may be improved when using the iodinated receptor **2**. Very recently, some halogen-bonding receptors based on I-PFCs were also developed for tightly binding halide anions in solution [46, 51]. Therefore, the use of iodinated macrocycles and I-PFCs is recommended as the basis for the design of halogen-bonding-based receptors. From Table 3, it is also clear that in the water environment, the observed order of halide ion affinity ($Br^- > Cl^- > I^-$) for the halogen-bonding receptors **1** and **2** is consistent with experimental results which show that receptor **1** exhibits an impressively high binding affinity for Br^-. Nonetheless, it must be pointed out that the titration experiments were carried out in competitive aqueous solvent media (9:1 CD_3OD/D_2O) while the present solution calculations were performed in water. This may

result in certain discrepancies between the theoretical results and experimental data.

Conclusions

In this work, quantum chemical calculations were performed at the DFT/B3LYP level on the anion complexes of **1–3**, which were selected as models to understand the binding behavior of macrocyclic receptors by bidentate halogen bonds and multiple hydrogen-bonding interactions. To justify the reliability of the B3LYP/cc-pVDZ method for describing the complexes under investigation, a preliminary and comparative study of the simple systems of the brominated ion pair **4** was carried out at the B3LYP and MP2 levels with the same or a larger basis set. It was shown that the B3LYP/cc-pVDZ calculations reliably predict the structures and relative order of affinity strengths of the X^- complexes.

For the halogenated receptors **1** and **2**, halide ions are held by two equivalent X...X^- interactions that are less linear than those in the small complexes of ion pair **4**. To accommodate the negatively charged guest anions, the structures of the halogen-bonding receptors **1** and **2** fully reorganize into a calix-like shape, attracting the two positively charged halogen atoms more closely. In the systems of the nonhalogenated receptor **3**, halide ions are involved in four hydrogen-bonding interactions: two C^2–H...X^- and two C^8–H...X^- hydrogen bonds. The major driving force for complexation between receptor **3** and halide ions comes from the two imidazolium C^2–H...X^- hydrogen bonds, while the two benzene C^8–H...X^- interactions also contribute to the binding of anions. When guest anions are present, both the imidazole and benzene rings in the hydrogen-bonding receptor **3** tend to point towards the anions and thus rotate to form a cage-like shape.

At the B3LYP/cc-pVDZ level, the interaction energies for the complexes under study span the range between −39.02 kcal mol^{-1} and −84.30 kcal mol^{-1}. In particular, as compared to the halogen-bonding receptors **1** and **2**, the computed interaction energies for the systems of the hydrogen-bonding receptor **3** show a decease in absolute value. Therefore, the binding affinities of anions in the gas phase strengthen with the addition of halogen atoms to the imidazole rings of the cyclophane receptor. Moreover, in the water environment, the calculated interaction energies of the complexes of **2** appear to be somewhat greater than those for the systems of **1** and **3**. In this regard, the binding affinities of the halide anions may be improved in solvent media when using the iodinated receptor **2**.

In summary, the incorporation of halogen atoms into the macrocyclic framework induces disparate conformations of the receptor to accommodate the halide ions as well as totally different binding behavior towards the anions, thus enabling halide ion recognition to take place via pure halogen-bonding interactions. Moreover, the binding affinities of the halide ions for the cyclophane receptor were found to be enhanced with the introduction of halogen atoms into functional groups of the receptor. The use of iodinated macrocycles and I-PFCs is recommended as the basis for the design of halogen-bonding-based receptors for anion recognition. Our ongoing efforts focus on investigating the binding behaviors of more complex receptors that possess multiple halogen-bond donors or hydrogen- and halogen-bond donors towards various guest anions such as NO_3^-, HSO_4^-, X^-, etc.

Acknowledgments This work was supported by the Natural Science Foundation of Shanghai (11ZR1408700), the National Natural Science Foundation of China (20736002 and 21103047), the Program for Changjiang Scholars and Innovative Research Team in the University of China (IRT0721), and the 111 Project of China (B08021).

References

1. Bianchi A, Bowman-James K, García-España E (1997) Supramolecular chemistry of anions. Wiley-VCH, New York
2. Sessler JL, Gale PA, Cho WS (2006) Anion receptor chemistry. Royal Society of Chemistry, Cambridge
3. Beer PD, Gale PA (2001) Angew Chem 113:502–532
4. Beer PD, Gale PA (2001) Angew Chem Int Ed 40:486–516
5. Fabbrizzi L, Licchelli M, Rabaioli G, Taglietti A (2000) Coord Chem Rev 205:85–108
6. O'Neil EJ, Smith BD (2006) Coord Chem Rev 250:3068–3080
7. Caltagirone C, Gale PA (2009) Chem Soc Rev 38:520–563
8. Chakrabarti P (1993) J Mol Biol 234:463–482
9. Kubik S (2009) Chem Soc Rev 38:585–605
10. Choi K, Hamilton AD (2003) Coord Chem Soc 240:101–110
11. Bondy CR, Loeb SJ (2003) Coord Chem Soc 240:77–99
12. Schmidtchen FP, Berger M (1997) Chem Rev 97:1609–1646
13. Kang SO, Begum RA, Bowman-James K (2006) Angew Chem Int Ed 45:7882–7894
14. Kang SO, Begum RA, Bowman-James K (2006) Angew Chem 118:8048–8061
15. Pal D, Suhnel J, Weiss MS (2002) Angew Chem Int Ed 41:4663–4666
16. Walton JD, Milner-White EJ (2002) J Mol Biol 315:183–191
17. Ledvina PS, Yao N, Choudhary A, Quiocho FA (1996) Proc Natl Acad Sci USA 93:6786–6791
18. Kubik S, Kirchner R, Nolting D, Seidel J (2002) J Am Chem Soc 124:12752–12760
19. Hudnall TW, Chiu CW, Gabbai FP (2009) Acc Chem Soc 42:388–397
20. Gamez P, Mooibroek TL, Teat SJ, Reedijk J (2007) Acc Chem Res 40:435–444
21. Hay BP, Bryantsev VS (2008) Chem Commum 2417–2428
22. Schottel BL, Chifotides HT, Dunbar KR (2008) Chem Soc Rev 37:68–83
23. Rosokha V, Lindeman SV, Rosokha SV, Kochi JK (2004) Angew Chem 116:4750–4752
24. Rosokha V, Lindeman SV, Rosokha SV, Kochi JK (2004) Angew Chem 43:4650–4652
25. Berryman OB, Hof F, Hynes MJ (2006) Chem Commun 506–508

26. Metrangolo P, Neukirch H, Pilati T, Resnati G (2005) Acc Chem Res 38:386–395
27. Metrangolo P, Meyer F, Pilati T, Resnati G, Terraneo G (2008) Angew Chem Int Ed 47:6114–6127
28. Cavallo G, Metrangolo P, Pilati T, Resnati G, Sansotera M, Terraneo G (2010) Chem Soc Rev 39:3772–3784
29. Bertani R, Sgarbossa P, Venzo A, Lelj F, Amati M, Resnati G, Pilati T, Metrangolo P, Terraneo G (2010) Coord Chem Rev 254:677–695
30. Politzer P, Murray JS, Clark T (2010) Phys Chem Chem Phys 12:7748–7757
31. Auffinger P, Hays FA, Westhof E, Ho PS (2004) Proc Natl Acad Sci USA 101:16789–16794
32. Lu YX, Wang Y, Zhu WL (2010) Phys Chem Chem Phys 12:4543–4551
33. Lu YX, Shi T, Wang Y, Yang HY, Yan YH, Luo XM, Jiang HL, Zhu WL (2009) J Med Chem 52:2854–2862
34. Parisini E, Metrangolo P, Pilati T, Resnati G, Terraneo G (2011) Chem Soc Rev 40:2267–2279
35. Politzer P, Lane P, Concha MC, Ma Y, Murray JS (2007) J Mol Model 13:305–311
36. Clark T, Hennemann M, Murray JS, Politzer P (2007) J Mol Model 13:291–296
37. Politzer P, Murray JS, Concha MC (2007) J Mol Model 13:643–650
38. Murray JS, Lane P, Politzer P (2009) J Mol Model 15:723–729
39. Murray JS, Riley KE, Politer P, Clark T (2010) Aust J Chem 63:1598–1607
40. Bernard-Houplain MC, Bourderon C, Peron JJ, Sandorfy C (1971) Chem Phys Lett 11:149–151
41. Favrot J, Leclercq JM, Roberge R, Sandorfy C, Vocelle D (1978) Chem Phys Lett 53:433–435
42. Cabot R, Hunter CA (2009) Chem Commun 2005–2007
43. Libri S, Jasim NA, Perutz RN, Brammer L (2008) J Am Chem Soc 130:7842–7844
44. Dimitrijevic E, kvak O, Tayor MS (2010) Chem Commun 9025–9028
45. Sarwar MG, Dragisic B, Salsberg LJ, Gouliaras C, Tayor MS (2010) J Am Chem Soc 132:1646–1653
46. Sarwar MG, Dragisic B, Sagoo S, Taylor MS (2010) Angew Chem Int Ed 49:1674–1677
47. Caballero A, White NG, Beer PD (2011) Angew Chem Int Ed 50:1845–1848
48. Serpell CJ, Kilah NL, Costa PJ, Felix V, Beer PD (2010) Angew Chem Int Ed 49:5322–5326
49. Kilah NL, Wise MD, Serpell CJ, Thompson AL, White NG, Christensen KE, Beer PD (2010) J Am Chem Soc 132:11893–11895
50. Kilah NL, Wise MD, Beer PD (2011) Cryst Growth Des 11:4565–4571
51. Chudzinski MG, McClary CA, Taylor MS (2011) J Am Chem Soc 133:10559–10568
52. Sessler JL, Camiolo S, Gale PA (2003) Coord Chem Rev 240:17–55
53. Wedge TJ, Hawthorne ME (2003) Coord Chem Rev 240:111–128
54. Best MD, Tobey SL, Anslyn EV (2003) Coord Chem Rev 240:3–15
55. Gale PA (2003) Coord Chem Rev 240:191–221
56. Blondeau P, Segura M, Perez-Fernandez R, de Mendoza J (2007) Chem Soc Rev 36:198–210
57. Schug KA, Lindner W (2005) Chem Rev 105:67–113
58. Schmuk C (2006) Coord Chem Rev 205:3053–3067
59. Schmuk C, Wich P (2006) Angew Chem Int Ed 45:4277–4281
60. Moiani D, Cavallotti C, Famulari A, Schmuck C (2008) Chem Eur J 114:5207–5219
61. Chen Y, Pan X, Yan H, Tan N (2011) Phys Chem Chem Phys 13:7384–7395
62. Xu Z, Kim SK, Yoon J (2010) Chem Soc Rev 39:1457–1467
63. Becke AD (1988) Phys Rev A 38:3098–3100
64. Lee C, Yang W, Parr RG (1988) Phys Rev B 37:785–789
65. Lu Y, Li H, Zhu X, Zhu W, Liu H (2011) J Phys Chem A 115:4467–4475
66. Dunning TH (1989) J Chem Phys 90:1007–1023
67. Boys SF, Bernardi F (1970) Mol Phys 19:553–566
68. Moller C, Plesset MS (1934) Phys Rev 46:618–622
69. Barone V, Cossi M, Tomasi J (1997) J Chem Phys 107:3210–3221
70. Tomasi J, Persico M (1994) Chem Rev 94:2027–2094
71. Tomasi J, Mennucci B, Cammi R (2005) Chem Rev 105:2999–3093
72. Frisch MJ, Trucks GW, Schlegel HB, Scuseria GE, Robb MA, Cheeseman JR, Montgomery JA Jr, Vreven T, Kudin KN, Burant JC, Millam JM, Iyengar SS, Tomasi J, Barone V, Mennucci B, Cossi M, Scalmani G, Rega N, Petersson GA, Nakatsuji H, Hada M, Ehara M, Toyota K, Fukuda R, Hasegawa J, Ishida M, Nakajima T, Honda Y, Kitao O, Nakai H, Klene M, Li X, Knox JE, Hratchian HP, Cross JB, Adamo C, Jaramillo J, Gomperts R, Stratmann RE, Yazyev O, Austin AJ, Cammi R, Pomelli C, Ochterski JW, Ayala PY, Morokuma K, Voth GA, Salvador P, Dannenberg, JJ, Zakrzewski VG, Dapprich S, Daniels AD, Strain MC, Farkas O, Malick DK, Rabuck AD, Raghavachari K, Foresman JB, Ortiz J V, Cui Q, Baboul AG, Clifford, S, Cioslowski J, Stefanov BB, Liu G, Liashenko A, Piskorz P, Komaromi I, Martin RL, Fox DJ, Keith T, Al-Laham MA, Peng CY, Nanayakkara A, Challacombe M, Gill PMW, Johnson B, Chen W, Wong MW, Gonzalez C, Pople JA (2004) Gaussian 03, revision C.02. Gaussian Inc., Wallingford
73. Bondi A (1964) J Phys Chem 68:441–451
74. Yan S, Cho SJ, Lee SJ, Kang S, Paek K, Lee JY (2008) Phys Chem Chem Phys 10:7079–7084
75. Bandyopadhyay I, Raghavachari K, Flood AH (2009) Chem Phys Chem 10:2535–2540
76. Bazzicalupi C, Bencini A, Bianchi A, Danesi A, Giorgi C, Lorente MAM, Valtancoli B (2006) New J Chem 30:959–965
77. Zuo S, Quan JM, Wu Y (2007) Org Lett 9:4219–4222
78. Pedzisa L, Hay BP (2009) J Org Chem 74:2554–2560
79. Bryantsev VS, Hay BP (2005) J Am Chem Soc 127:8282–8283
80. Bryantsev VS, Ha BP (2005) Org Lett 27:5031–5034